Earthq Eng & Eng Vib (2024) 23: 359-376 **DOI**: https://10.1007/s11803-024-2241-0

Pile foundation in alternate layered liquefiable and non-liquefiable soil deposits subjected to earthquake loading

Praveen Huded M[1†] and Suresh R Dash[2‡]

1. *LEA Associates South East Asia Pvt. Ltd., New Delhi 110044, India*
2. *Indian Institute of Technology Bhubaneswar, Khurda 752050, India*

Abstract: Pile foundations are still the preferred foundation system for high-rise structures in earthquake-prone regions. Pile foundations have experienced failures in past earthquakes due to liquefaction. Research on pile foundations in liquefiable soils has primarily focused on the pile foundation behavior in two or three-layered soil profiles. However, in natural occurrence, it may occur in alternative layers of liquefiable and non-liquefiable soil. However, the experimental and/or numerical studies on the layered effect on pile foundations have not been widely addressed in the literature. Most of the design codes across the world do not explicitly mention the effect of sandwiched non-liquefiable soil layers on the pile response. In the present study, the behavior of an end-bearing pile in layered liquefiable and non-liquefiable soil deposit is studied numerically. This study found that the kinematic bending moment is higher and governs the design when the effect of the sandwiched non-liquefied layer is considered in the analysis as opposed to when its effect is ignored. Therefore, ignoring the effect of the sandwiched non-liquefied layer in a liquefiable soil deposit might be a nonconservative design approach.

Keywords: pile foundation; liquefaction; alternately layered soil; fixity effect; layered effect

1 Introduction

Pile foundations are still one of the most common deep foundation systems for high-rise buildings, particularly when the soil supporting the foundation is weak. Pile foundations have prevented the complete collapse of buildings during earthquakes (e.g., Niigata earthquake of 1964). However, many buildings and bridges have shown major damage during past earthquakes due to liquefaction (Hamada and O'Rourke, 1992; Yoshida *et al*., 2007). The pile foundation in liquefiable soil is a transient problem involving superstructure and pile foundation's inertial interaction, reduction of soil strength, and development of excess pore water pressure due to dynamic load (Berrill and Yasuda, 2002; Liyanapathirana and Poulos, 2005; Wang *et al*., 2017). Failure of pile foundations has been observed in both level and sloping ground (Finn and Fujita, 2002). Zhang and Yang (2018) carried out shake table tests to understand the pile failure mechanism due to the lateral spreading of the frozen ground crust due to the liquefaction of subsoil layers. Pile foundations in liquefiable soil may fail because of bending, buckling, shear, or settlement failure (Mohanty *et al*., 2017, 2021). The post-earthquake effects studied through excavations revealed the formation of plastic hinges in the pile foundation at the interface of the soil layer (Tokimatsu and Asaka, 1998; Yoshida and Hamada, 1990). Early research emphasized kinematic bending as a reason for pile failures (Hamada and O'Rourke, 1992; Yoshida *et al*., 2007; Yoshida and Hamada, 1990). JRA (2003), FEMA 369 (2000), and CEN (2004) are the design guidelines available for the design of pile foundations in potentially liquefiable soil deposits. Despite these guidelines, the failure of pile-supported structures has been reported. These failures indicate that the design guidelines do not include all the underlying failure mechanisms (Bhattacharya, 2003). Berrill and Yasuda (2002) highlighted the possibility of a buckling failure mechanism. Once the soil liquefies, the pile will act as a slender member without the soil support, axial and horizontal load from the superstructure affects the lateral stiffness of the pile foundation. Many researchers have demonstrated the buckling failure mechanism through experimental and numerical approaches (Bhattacharya, 2003; Bhattacharya *et al*., 2005; Haldar *et al*., 2008; Haldar and Babu, 2010; Dash *et al*., 2010; Knappett and Madhabhushi, 2009).

Many experiments (small scale and full scale) have been carried out by researchers that helped in understanding the behavior of pile foundations in

Correspondence to: Suresh R Dash, Indian Institute of Technology Bhubaneswar, Aragul, Jatni, Khurda 752050, India
Tel.: +91 80183 55444
Email: srdash@iitbbs.ac.in; ph01@iitbbs.ac.in
[†]Senior Engineer; [‡]Assistant Professor
Received April 22, 2022; **Accepted** June 29, 2023

liquefiable soil. Some of the notable studies were carried out by Wilson (1998), Ashford and Juirnarongrit (2002), Abdoun *et al*. (2003), Brandenberg *et al*. (2005), Knappett and Madabhushi (2009), Tang *et al*. (2010, 2016), Zhang and Yang (2018), Wang *et al*. (2019b), Dash and Bhattacharya (2021), Zhang *et al*. (2022b), Wang *et al*. (2023), and Zhang *et al*. (2022a). Various numerical tools have also been used to simulate pile behavior in liquefiable soil ranging from a simplified 1D model to a complex two/three-dimension model. To cite a few, Chang and Jemeric (2009), Tang *et al*. (2014), Wang and Orense (2020) used two and three-dimensional complex finite element methods. However, because of the simplicity of 1D analysis, several researchers used the pseudo-static method and beam on nonlinear Winkler foundation (BNWF) method (Zhang *et al*., 2008; Cubrinovski *et al*., 2009; Janalizadeh and Zahmatkesh, 2015; Liyanapathirana and Poulos, 2005; Wang *et al*., 2017; Hui *et al*., 2018; Jia *et al*., 2023). In the BNWF method, the pile-soil interaction is modelled using *p-y* springs, which are obtained from field tests (Liyanapathirana and Poulos, 2005; Zhang and Yang, 2018). The pile-soil interaction represented in this method depends on pile-soil relative displacement at a particular depth and does not depend on soil resistance above and below Wilson (1998). Most of these experimental and numerical studies were restricted to two-layered (top liquefiable soil layer) or three-layered soil deposits (non-liquefiable soil deposit with a sandwiched liquefiable soil layer).

Pile foundations for bridges and buildings often pass through liquefiable and non-liquefiable soil deposits. Also, the natural occurrence of soil layers may occur in alternate layers (e.g., a liquefiable soil deposit with a sandwiched non-liquefiable soil layer). To the best of the authors' knowledge, experimental and numerical studies concerning the response of pile foundations in alternate layers are scarce. JRA (2003) code has given several recommendations to consider the lateral pressure applied by the liquefiable soil deposit on the pile foundation. However, the code does not comment on the consideration of lateral pressure applied by the sandwiched non-liquefiable soil layer on the pile foundation. The sandwiched non-liquefiable soil layer, if it exists in the liquefiable soil deposit, would create a stiffness contrast at the interface of the soil layers and would alter the pile response. Bhattacharya and Goda (2013) have stated that a relatively thin non-liquefiable soil layer (of thickness 5-6*D*) may not offer restraint to the pile. A sandwiched non-liquefiable layer of thickness greater than 9*D* would give significant lateral restraint to the pile; however, these are mere estimations suggested by the author which require further studies. In the present study, an attempt is made to understand the pile response in alternate layered liquefiable and non-liquefiable soil deposits using the numerical modelling approach. A two-dimensional numerical model is developed and validated against centrifuge test data. A detailed parametric study has been carried out by subjecting the model to earthquake time history with varied scaled earthquake amplitudes and frequencies.

2 Pile foundation in alternate layered liquefiable and non-liquefiable soil profile

The soil profiles considered in the study are shown in Fig. 1. Soil profile (a) is the standard case without any sandwiched non-liquefiable (clay) soil layer along with a schematic representation of the pile foundation. In other soil profiles, layer-1 (from top) is a liquefiable sandy soil with a relative density (D_r) of 35%, Layer-2 is a non-liquefiable clay layer, and different types of clays (soft, medium, and stiff) with varying thickness are considered in the study. The properties of the clay layer are chosen based on the recommendations of IS 2911 (2010). Layer-3 is again a liquefiable sandy soil with a relative density (D_r) of 35%, and the bottom layer is a very dense sandy soil with a relative density of (D_r) 80%. An end-bearing steel pile with a length of 24 m in which 22 m is embedded in the soil. The pile head is 2 m above the ground level with a superstructure mass of 100 t. The outside diameter of the pile is 0.67 m, and the wall thickness of the pile is 72 mm. The yield and ultimate moment capacity of the pile is M_y= 4577 kN·m (yield stress 250 N/mm^2) and M_c= 7503 kN·m (ultimate stress 410 N/mm^2), respectively. The Kobe earthquake (1995) motion (predominant frequency 2.86 Hz) is used as an input earthquake motion. The earthquake resulted in extensive soil liquefaction and caused damage to piles under warehouses and harbor structures (Soga, 1998). Figure 2 shows the plot of the Kobe earthquake time

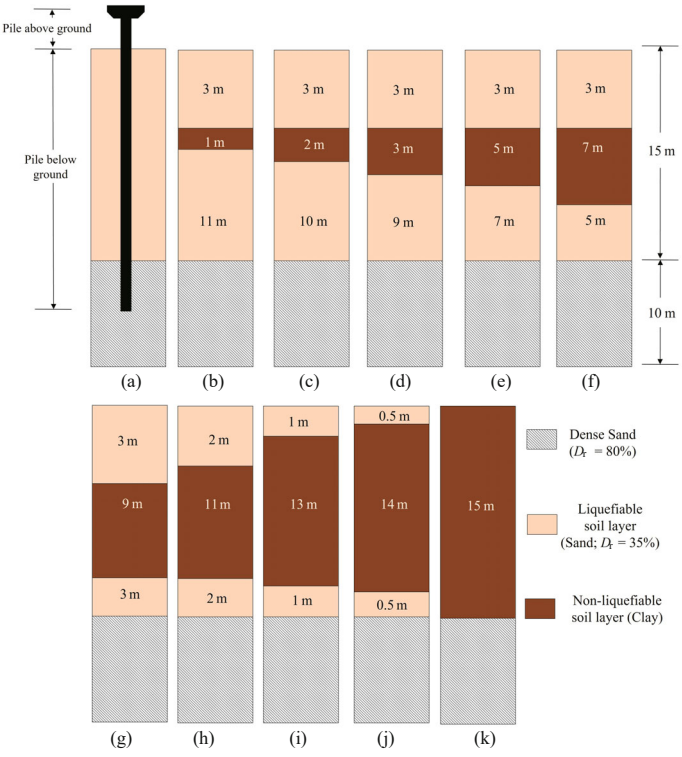

Fig. 1 Soil profiles considered in the study

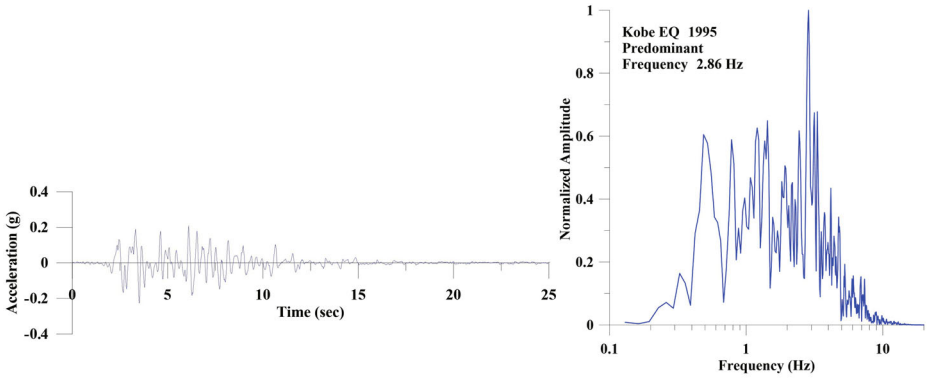

Fig. 2 Kobe earthquake time history plot and Fourier transform

history and its Fourier transform. The input motion is linear base corrected and scaled to 0.1 g, 0.2 g, 0.3 g, and 0.4 g to study the effect of PGA. The impact of parameters such as liquefiable and non-liquefiable soil, the position of the non-liquefiable soil layer in the liquefiable soil deposit, frequency of the input motion, and superstructure mass on the behavior of the pile foundation are studied.

2.1 Finite element modeling

The soil-pile system described above is modelled in OpenSees (Mckenna, 2011). Figure 3 shows the schematic illustration of the numerical model. The soil column is modelled as a plane strain element (2-D element). Soil is modelled with fine mesh in the vertical direction (0.5 m). The dimension of the soil column is fixed after the convergence study. A detailed description of the constitutive models is given below.

2.2 Soil models for liquefiable and non-liquefiable soil

Pressure-dependent multi-yield (PDMY) and pressure independent multi-yield (PIMY) constitutive material models are used to model sand (liquefiable soil) and non-liquefiable clay layer, respectively. The PDMY material simulates liquefaction under cyclic excitation (Yang, 2000). Four-node QuadUP elements are used to simulate solid-fluid coupled material response under cyclic excitation (Biot, 1955), and the constitutive soil model is defined. Tables 1(a) and 1(b) show the soil properties of the constitutive material model considered in the analysis. These material models and elements have also been validated against the experimental results in studies by Yang *et al*. (2003), Wang *et al*. (2013), and Wang *et al*. (2017).

2.3 Soil pile interaction springs (*p-y* springs for sand and clay layer)

The relative displacement of the soil and pile and the contact reaction is modelled as cyclic nonlinear elastic springs (*p-y* springs), which are added to the model as a zero-length element connecting the soil node and the pile node. These spring properties are modified depending on the level of pore water pressure in the soil at various depths at each instant of the analysis. A similar scheme of a coupled soil-pile FE modelling approach with *p-y* curves was used by Wang *et al*. (2013), Wang *et al*. (2017), Wang *et al*. (2019a), Li and Motamed (2017) to verify the soil pile response in the experimental study. The studies have demonstrated that the coupled soil-pile FE modelling approach, like the present one, was able to capture pile behavior. The *p-y* springs for liquefiable sand were modelled by PyLiq1 (Wang *et al*., 2017). The

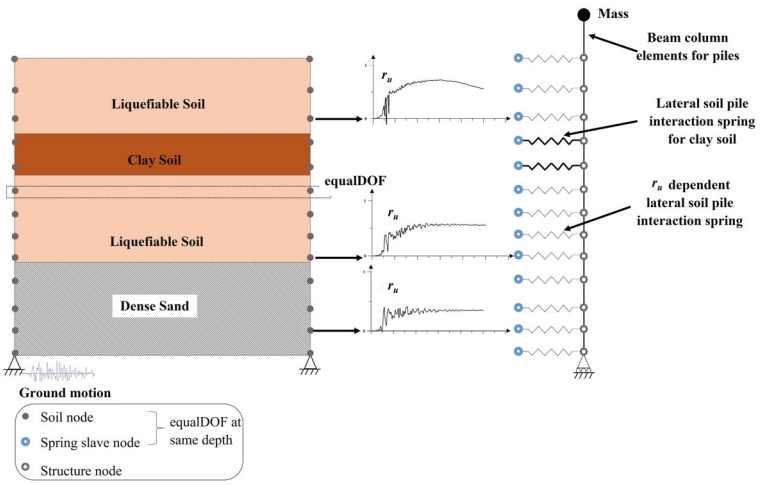

Fig. 3 Finite element model

Table 1(a) Soil properties of liquefiable soil

Pressure dependent multi yield material				
Relative density, D_r	**35%**	**45%**	**55%**	**80%**
Corrected SPT value, $(N_1)_{60}$	7	13	19	38
Specific gravity, G_s	3.0	2.65	2.65	2.65
Min. void ratio, e_{min}	1	0.52	0.52	0.52
Max. void ratio, e_{max}	1	0.89	0.89	0.89
Void ratio, e	0.76	0.73	0.68	0.59
Bulk density, ρ (t/m^3)	1.95	1.85	1.98	2.04
Friction angle, Φ	33	33.6	34.3	37
Reference pressure, $P_{resreff}$ (kPa)	80	80	80	80
Shear wave velocity, V_s (m/s)	151	166	181	215
Maximum shear modulus, G_{max} (kPa)	3.8×10^4	5.1×10^4	6.5×10^4	9.4×10^4
Octahedral ref. shear modulus, $G_{max,oct}$ (kPa)	4.7×10^4	6.2×10^4	7.9×10^4	1.1×10^4
Empirical poison's ratio, θ	0.33	0.33	0.33	0.33
Bulk modulus to shear modulus, B/G	3	2.67	2.67	2.67
Bulk modulus, B_r (kPa)	1.2×10^5	1.6×10^5	2.1×10^5	3.1×10^5
Pressure dependent coefficient, d_p	0.5	0.5	0.5	0.5
Contraction, c	0.039	0.033	0.028	0.019
Dilation coefficient, d_1	0.4	0.4	0.4	0.6
Dilation coefficient, d_2	2	2	2	3
Liq_1	10	10	10	5
Liq_2	0.01	0.01	0.01	0.003
Liq_3	1	1	1	1

Liq_1 define the effective confining pressure below which is in effect; Liq_2 and Liq_3 control the plastic shear strain accumulation (i.e., cyclic mobility).

Table 1(b) Properties of non-liquefiable clay soil

Pressure independent multi-yield material			
Clay	**Soft**	**Medium**	**Stiff**
Undrained shear strength, S_u (kPa)	21	43	87
Saturated density, ρ (t/m^3)	1.3	1.5	1.8
Cohesion, C_u (kPa)	18	37	75
Reference pressure of clay model, f_{reff} (kPa)	100	100	100
Maximum shear modulus, $G_{max,c}$ (kPa)	14546	29904	60620
Octahedral ref. shear modulus, $G_{max,c,oct}$ (kPa)	14546	29904	60620
Max shear strain, $\gamma_{max,c}$	0.1	0.1	0.1
Empirical poison's ratio, θ_c	0.41	0.41	0.41
B/G	5.2	5.2	5.2
Bulk modulus, B_r	75930.0	156099.0	316436.0
Pressure dependent coeff., d_c	0	0	0
Friction angle, φ	0	0	0
Number of yield surfaces	20	20	20
k_c (m/s)	1×10^{-9}	1×10^{-9}	1×10^{-9}

ultimate strength $p_{ult,liq}$ changes with the development of the excess pore water pressure ratio (r_u) as per the following equation.

$$p_{ult,liq} = p_{ult}\left(1 - r_u\right) + p_{res} r_u \quad (1)$$

where $r_u = \Delta u/\sigma'_y$, σ'_v is effective overburden pressure (kPa) at the measured point and Δu (kPa) is the excess pore water pressure developed as a result of earthquake load. The residual strength of the *p-y* curve is given by $p_{res} = m_p \times p_{ult}$ where m_p is a reduction factor based on the developed excess pore water pressure given by Brandenberg *et al*. (2005). The ultimate strength of the *p-y* curve p_{ult} (kN/m) is a function of the pile diameter *D* (m), effective unit weight of the soil, and depth below the ground level *z* (*m*) (API, 2005). The *p-y* relation is given as per the following equation (Parker and Reese, 1970).

$$p = A p_{ult,liq} \tanh\left(\frac{n_h z}{A p_{ult,liq}} y\right) \quad (2)$$

where *A* is the loading factor, and n_h is the rate of increase of the horizontal subgrade modulus and depends on the friction angle of the soil. Overburden correction is used for soil at greater depth, according to Boulanger *et al*. (1999). For the non-liquefiable clay layer, the PySimple1 spring is used to model lateral pile-soil interaction (see Boulanger *et al*., 1999). Since the effective stress in the clay layer does not change during the earthquake loading, the p_{ult} is assigned a constant value (Wang *et al*., 2017). The *p-y* curves for clay soil can be generated based on the API (2005) guidelines, which are based on the model proposed by Matlock (1970) as given below.

$$p = \frac{1}{2} p_{ult,c} \left[\frac{y}{2.5 D \varepsilon_{50}}\right]^{\frac{1}{3}} \quad (3)$$

where ε_{50} is the strain at half the maximum principal stress difference, and different values are recommended for soft, medium, and stiff clay soils.

2.4 Pile model

In general, piles and structures are modelled based on their performance in experiments as either elastic or inelastic elements. The validation model chosen (details of the validation are explained in the next section) from centrifuge tests had the pile response within a linear elastic zone. Therefore, here the pile is modelled using elastic beam-column elements. For further parametric study, the pile element is also kept elastic, and its performance is monitored. The superstructure mass is assigned as the lumped mass on the pile head. While evaluating the inertial bending moments in the pile, the lumped pile head mass is considered. Whereas, while evaluating the kinematic bending moment of the pile, pile head mass is ignored to isolate the situation of relative soil movement around pile foundation. The pile is meshed at 0.5 m so that it is not consistent with the vertical mesh of the soil. The pile considered for the study is a free head pile.

2.5 Solution method and boundary condition adopted

The pure shear condition, which is achieved through the laminar shear box in centrifuge tests, is achieved by obtaining equal degrees of freedom to the nodes at the same level. The soil nodes other than the nodes at the surface are made impervious, and the nodes at the surface are enabled to drain. The bottom soil nodes are fixed in the horizontal and vertical directions, as shown in Fig. 3. The Krylov-Newton algorithm and Newmark integrator are adopted in the numerical model. Rayleigh damping with mass and stiffness proportional damping is adopted.

2.6 Validation of developed finite element model against centrifuge test

In the present study, one of the experiments from the centrifuge tests carried out by Wilson (1998) has been considered for verification. The experimental model named Csp3-J is numerically modelled using OpenSees®. The experimental setup of Csp3-J consists of a two-layered soil (saturated uniformly graded Nevada sand) with the top layer being liquefiable (as shown in Fig. 4). The experimental model in the prototype scale has the thickness of the topsoil layer as 9.3 m with 55% relative density and the bottom soil layer thickness as 11.4 m with 80% relative density. An instrumented steel pipe pile with a diameter of 0.67 m and 72 mm wall thickness was used. The pile head was 3.81 m above the ground level with a mass of 49.1 Mg. The pile was embedded 16.7 m into the soil. The Kobe earthquake of 1995 was given as an input motion to the centrifuge (Fig. 2). A numerical model (FE based) for this centrifuge experiment is prepared in prototype scale, as shown in Fig. 4. The constitutive models used for modelling both the soil layers are listed in Table 2.

2.6.1 Result comparison

The results in terms of development of excess pore water pressure, soil acceleration, and bending moment of the pile obtained from the present numerical model is compared with that being observed in the experimental centrifuge model study (Fig. 5). The excess pore water pressure and acceleration in the soil of the numerical model are found to match fairly well with the centrifuge test results. The time-history patterns of pile bending moment also match quite well with the observation, with a maximum difference of 9.16% for the peak response in comparison with the centrifuge results. Predicting the dynamic response reasonably well, the developed numerical model can therefore be considered reasonable for further analysis of the pile foundation in liquefiable soil. This numerical modelling scheme is taken further for parametric study for the present scope of the work and presented in the following sections.

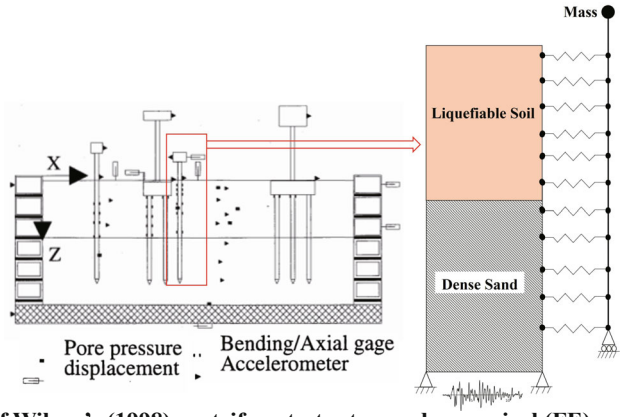

Fig. 4 Layout of Wilson's (1998) centrifuge test setup and numerical (FE) model developed in this study

Table 2 Soil properties used in the validation

Soil elastic properties	Top layer	Bottom layer	Reference
Relative density, D_r	55%	80%	-
Saturated mass density (Mg/m^3)	2.67	2.67	Haldar and Babu (2010)
Reference pressure (kPa)	80.0	80.0	-
Pressure dependent coefficient	0.50	0.50	-
Shear modulus, G_{max} (MPa)	65.0	94.1	Hardin and Drnevich (1972)
Bulk modulus, K_{max} (MPa)	212	307	Haldar and Babu (2010)
Peak shear strain (%)	10.00	10.00	-
Friction angle	33°	37°	Haldar and Babu (2010)
Material constants			-
C	0.0278	0.0188	
d_1	0.4	0.6	-
d_2	2	3	-
Liq_1	10	5	-
Liq_2	0.1	0.003	-
Liq_3	1	1	-

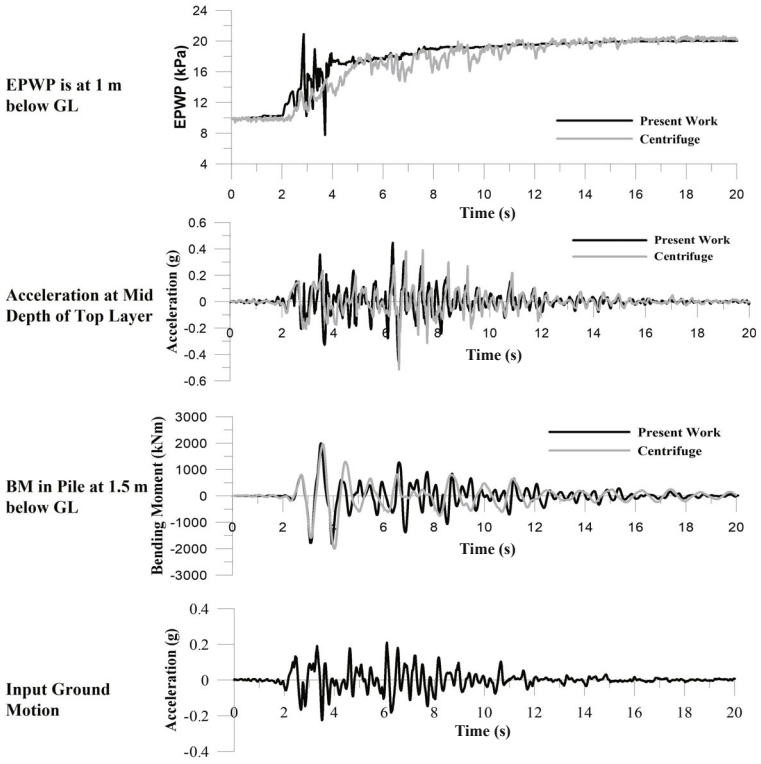

Fig. 5 Validation results of the numerical model

3 Results and discussion

3.1 Effect of sandwiched non-liquefiable soil layer on bending moment of the pile foundation

The developed numerical model is subjected to the Kobe earthquake (PGA scaled to 0.2 g), and the bending moment of the pile foundation is recorded at various times of loading for the soil profile cases considered in the study (Fig. 1). Figure 6 shows the variation normalized maximum bending moment (M_{max}/M_y) with the depth for several of the soil profile cases considered in Fig. 1. The location of the non-liquefiable soil layer is highlighted. It can be observed from Fig. 6 that the presence of sandwiched non-liquefiable soil significantly alters the bending moment of the pile at the boundary of the soil layers and is directly influenced by the type and thickness of the non-liquefiable soil layer. The bending moment changes its sign at each boundary layer of the soil, similar to the observations being made by Abdoun *et al*. (2003) and Janalizadeh and Zahmatkesh (2015). This change in bending moment profile along depth indicates the availability of partial fixity by the sandwiched non-liquefiable soil layers and high stiffness contrast at the soil interfaces. Note also that this partial fixity effect would decrease the effective length of the pile and hence would increase the buckling load-carrying capacity of the pile foundation in alternate layered soil deposits. In the present analysis, a soil layer of a depth of 1.5D would give a partial fixity effect in the case of medium and stiff clay as sandwiched non-liquefiable soil layers. However, for the case of soft clay, the soil layer of depth 7.5D (D – diameter of the pile) is required to obtain the partial fixity effect. Hence, if a non-liquefiable soil layer of sufficient strength and depth is encountered in the liquefiable soil deposit, then the layered effect must be considered in the analysis of the pile foundation. The depth of fixity for the piles embedded in liquefied soil is affected mainly by the depth of liquefaction and soil stiffness degradation ratio (Lombardi *et al*., 2010). The evaluation of the extent of liquefaction depth is largely a function of seismic excitation (Bhattacharya and Goda, 2013). The depth at which a pile could be assumed to be fixed below the depth of liquefied soil depends on the relative stiffness between the pile and soil (Davisson and Robinson, 1965). Also, a study by Zhang *et al*. (2020) showed an increase in the buckling capacity of the pile foundation in liquefied soil as the flexural stiffness of the pile increases. Therefore, it can be inferred that the fixity effect depends on the characteristics of the input ground motion and pile-soil stiffness.

3.2 Effect of sandwiched non-liquefiable soil layer on the maximum displacement of the pile foundation

The displacement profile of the pile subjected to Kobe earthquake motion scaled to 0.2 g is estimated for several of the soil profile cases considered in Fig. 1 and are presented in Fig. 7. The figure shows the plot of the normalized maximum pile displacement with depth.

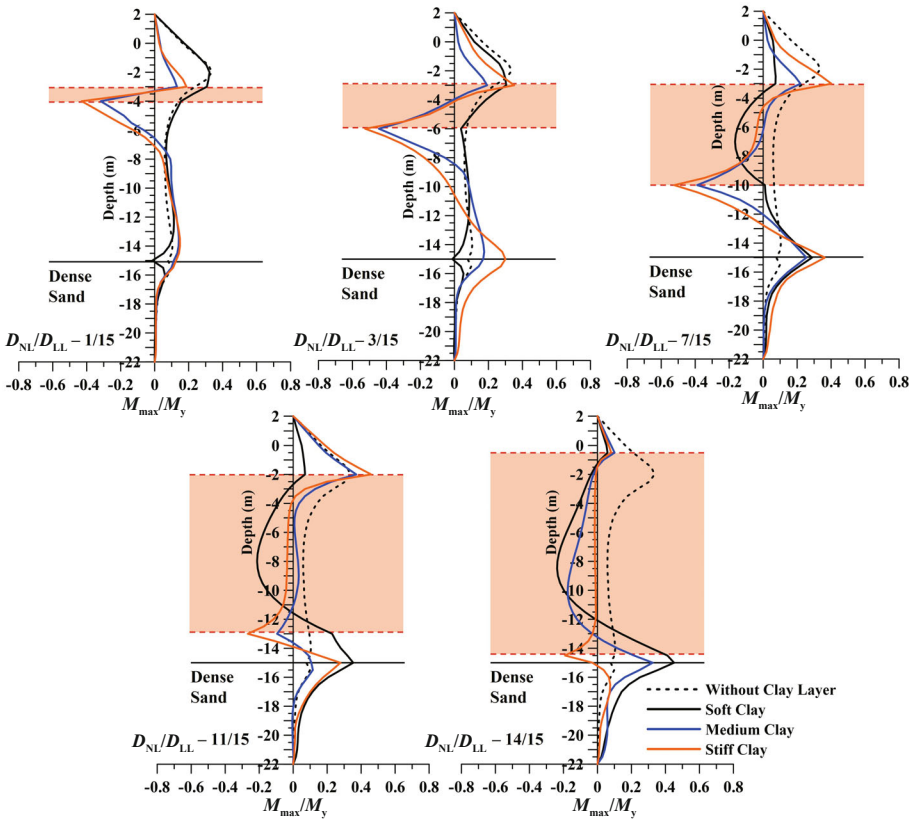

Fig. 6 Variation of normalized maximum bending moment profile (M_{max}/M_y) with depth for all the soil profiles

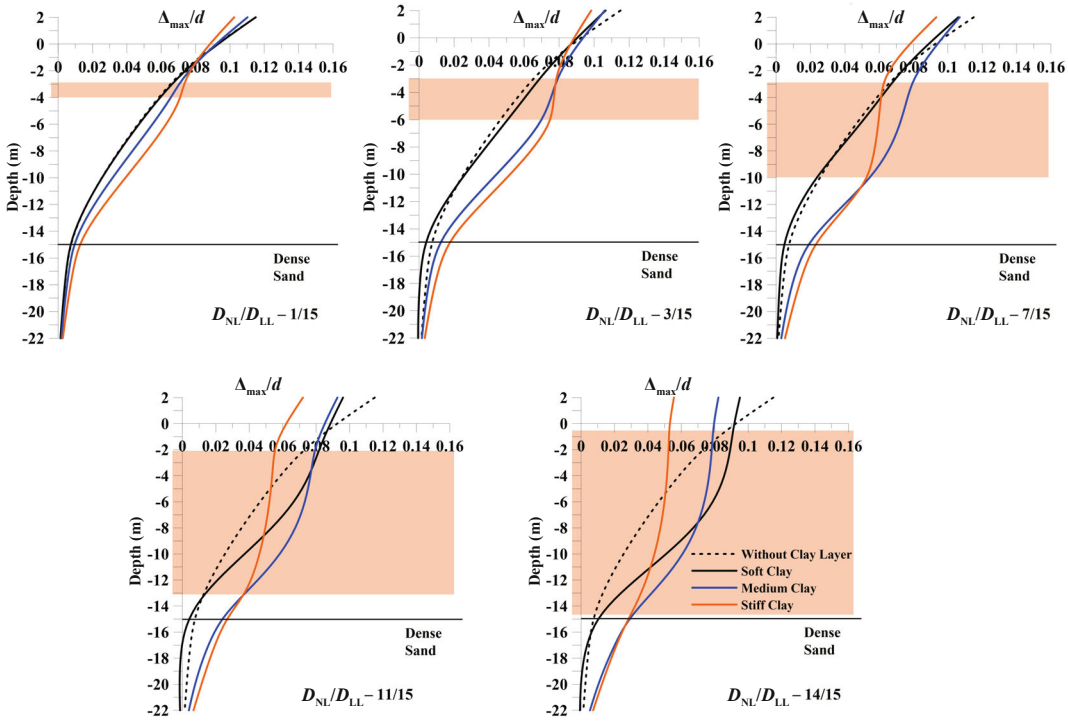

Fig. 7 Variation of normalized maximum pile displacement with depth

As can be observed from Fig. 7, there is no variation in displacement across the depth of the non-liquefiable clay layer for stiff clay of thickness 5 m and above, which indicates that the clay layer acts firm and moves as a block. The pile head displacement decreases as the thickness of the sandwiched non-liquefiable soil layer increases in the liquefiable soil deposit and is significant for the case of stiff clay, as shown in Fig. 8. Figure 9 shows the plot of the ratio of normalized maximum pile head displacement for all the soil profiles. As the ratio of the thickness of non-liquefiable soil to the thickness of liquefiable soil deposit (D_{NL}/D_{LL}) increases, the maximum pile head displacement is reduced by 18%, 29%, and 53% for the case of soft, medium, and stiff clay, respectively, as compared to the soil case without any sandwiched clay layer. However, it can be observed

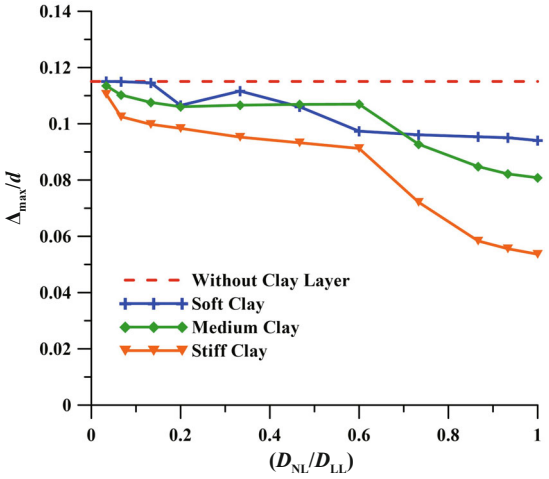

Fig. 9 Variation of normalized maximum pile head displacement for all soil profiles

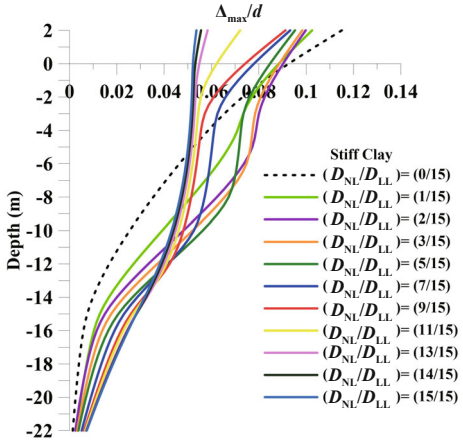

Fig. 8 Variation of normalized maximum displacement of the pile for the case of stiff clay of all thickness

that soft and medium clay soil layers are less effective in resisting the pile head displacement compared to stiff clay. The study indicates that the sandwiched non-liquefiable clay layer of sufficient strength and thickness resists the pile displacement and hence increases the load-carrying capacity of the pile against buckling during liquefaction.

3.3 Effect of peak ground acceleration on the maximum bending moment of pile foundation

To investigate the influence of the amplitude of ground acceleration on the bending moment of the pile foundation, Kobe earthquake ground motion scaled to different PGA values (0.1 g, 0.2 g, 0.3 g, and 0.4 g) is applied at the base of the soil layer. Figures 10 and 11 show

the plots of the variation of the normalized maximum bending moment for the case of D_{NL}/D_{LL}=0/15 and D_{NL}/D_{LL}=5/15, respectively. It can be observed from Fig. 10 that PGA values have a direct influence on the inertial bending moment of the pile foundation.

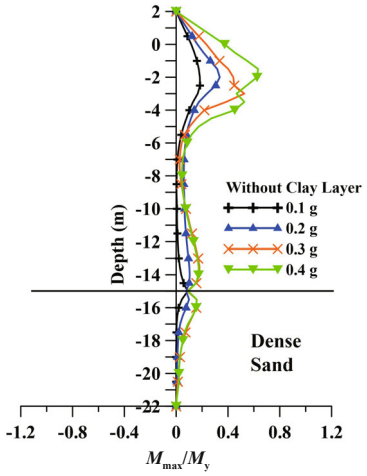

Fig. 10 Variation of the normalized maximum bending moment for the soil profile without any clay layer

However, for the case of soil deposits with the sandwiched clay layer (non-liquefied), as the strength of this non-liquefiable layer increases, inertial and kinematic bending moments increase with the increase in PGA values. Inertial bending moments are evaluated considering a lumped pile head mass. While evaluating the kinematic bending moment of the pile, no pile head mass was considered in the analysis so that the relative soil movement around the pile foundation was isolated. It can also be observed from Fig. 12 that at higher PGA values, the kinematic bending moment governs the pile design. Hence, neglecting the presence of the sandwiched clay layer might result in an underestimation of the kinematic bending moment at the boundary of the soil layers.

3.4 Investigation of the interaction of kinematic response and inertial response of pile

Deep foundations must be analyzed for combined kinematic and inertial loads (see Cubrinovski *et al.*, 2009). The magnitude of soil deformation and the soil stiffness during the earthquake load governs the kinematic loading on the pile. Figure 13 shows the

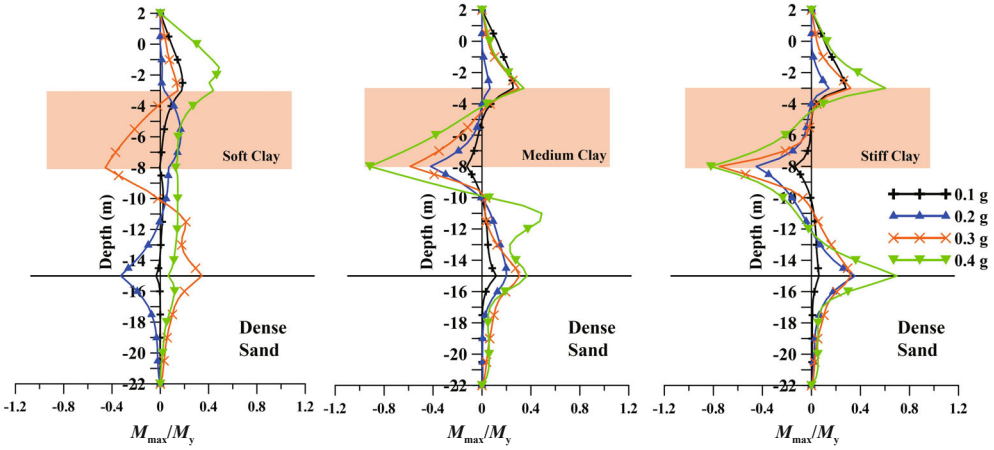

Fig. 11 Variation of the normalized maximum bending moment for different types of non-liquefiable clay layers with respect to different PGA values for the case of D_{NL}/D_{LL}–5/15

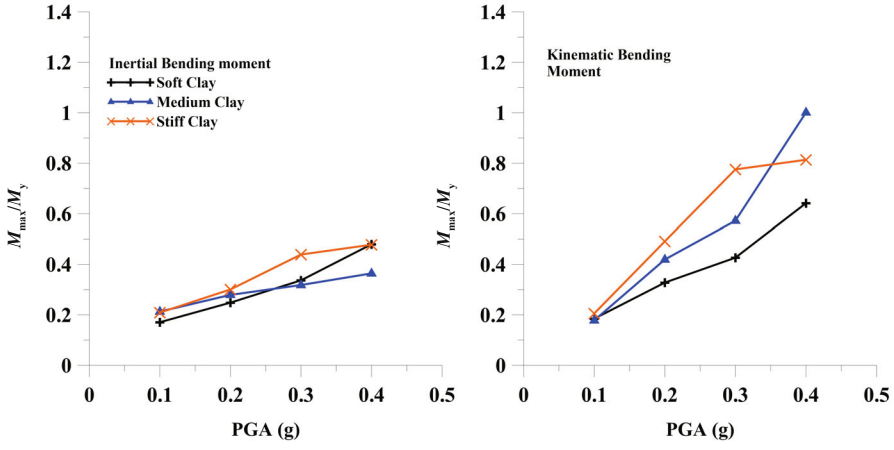

Fig. 12 Variation of the maximum inertial and kinematic bending moment for different types of non-liquefiable clay layers with respect to different PGA values for the case of D_{NL}/D_{LL}–5/15

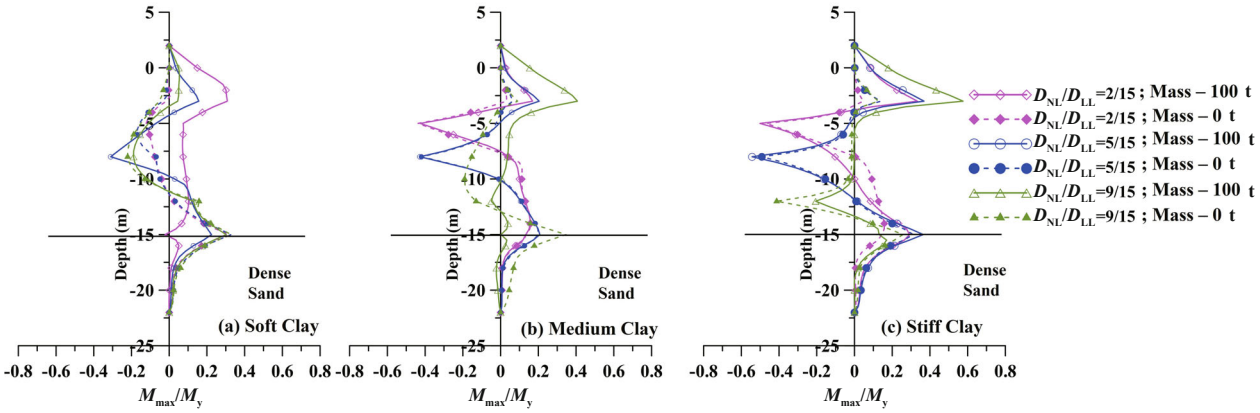

Fig. 13 Variation of the normalized maximum bending moment with depth (with superstructure mass and without superstructure mass)

plot of the variation of the ratio of the normalized maximum bending moment with depth for the case with superstructure mass (100 t) and without superstructure mass (0) for different types and thicknesses of the sandwiched clay layer. It observed from the study that the inertial effects largely concentrate at the top portion of the pile, whereas at deeper depths, the maximum bending moment occurs due to the kinematic loading. Several representative cases are shown in Fig. 13. For the depth of the non-liquefiable soil layer (medium and stiff) up to 7 m, the kinematic bending moment changes by a maximum of 15% due to consideration of inertial load. However, this change is 45.4% for stiff clay soil layers with a thickness of 9 m. Hence, for soil deposits with sandwiched clay layers of a smaller thickness (up to 10*D*), the influence of inertial loading on the kinematic bending moment is less. Therefore, for pile design in layered soil deposits, the kinematic bending moment must be considered. Figure 14 shows the type of bending moment which governs the design of pile foundations. From the figure, it can be suggested that for pile foundation in layered soil deposits, the design moment should be estimated considering both inertia and kinematic bending simultaneously as noted by Tokimatsu *et al*. (2005) and Xu *et al*. (2023).

D_{NL}/D_{LL}	Type of sandwiched clay layer		
	Soft Clay	Medium Clay	Stiff Clay
1/15	Kinematic	Kinematic	Kinematic
2/15	Kinematic	Kinematic	Kinematic
3/15	Kinematic	Kinematic	Kinematic
5/15	Kinematic	Kinematic	Kinematic
7/15	Kinematic	Kinematic	Kinematic
9/15	Kinematic	Inertial	Inertial

Fig. 14 Type of bending moment governing the design of pile foundation

3.5 Effect of frequency of input earthquake motion on maximum bending moment of the pile foundation

The pile response is governed by the frequency of the input earthquake motion (Haldar *et al*., 2008). To study the effect of frequency on the soil-pile system, a ground motion is applied as a sinewave (magnitude of 0.05 g) with various frequencies (0.1 Hz, 0.3 Hz, 0.5 Hz, 0.7 Hz, 1.0 Hz, 4.0 Hz, and 10 Hz) at the base of the soil layer. Figure 15 shows the plots of variation of the normalized maximum bending moment of the pile foundation for different types of soil profiles for different input frequencies. The pile response is much less at lower and higher frequency ground motions. However, when the input ground motion of frequency

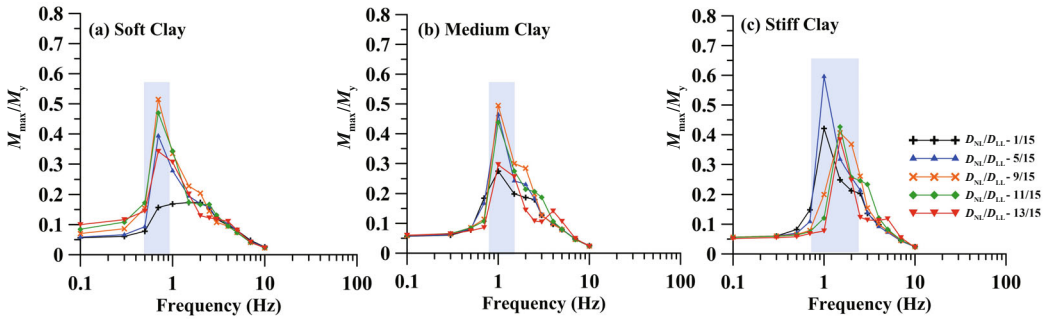

Fig. 15 Variation of the normalized maximum bending moment to yield moment vs frequency of input motion

is in the range 0.7 Hz–2.0 Hz, the response of the soil-pile system is maximum. This indicates that the soil-pile system considered has a natural frequency in the range of 0.7 Hz–2.0 Hz.

3.6 Effect of variation in superstructure mass

The effect of superstructure mass is studied, and the bending moment response for the case of the Kobe earthquake input motion (scaled to 0.2 g) is presented. The case of D_{NL}/D_{LL}= 5/15, corresponding to different types of sandwiched non-liquefiable clays, is studied. Figure 16 shows the variation of normalized maximum pile bending moment with the change in the pile head mass. It can be observed from the figure that with the increase in pile head mass, the inertial bending moment increases. However, the maximum kinematic bending moment at the bottom of the clay layer is not influenced by the superstructure mass, since the influence of the inertial effect induced by the pile head mass diminishes at deeper depths (Simonelli *et al*., 2014).

3.7 Effect of initial relative density of liquefiable soil

In all the analyses carried out except the one described in this section, the relative density of the liquefiable soil in layers 1 and 3 are considered as 35%. To investigate the effect of the initial relative density of the liquefiable soil layer on pile response, the relative densities of soil layers 1 and 3 are varied. The variation of normalized bending moment of the pile foundation for different relative densities of liquefiable soil is shown in Fig. 17 (Kobe earthquake scaled to 0.2 g) for the soil profiles shown in Figs. 1(a) and 1(e).

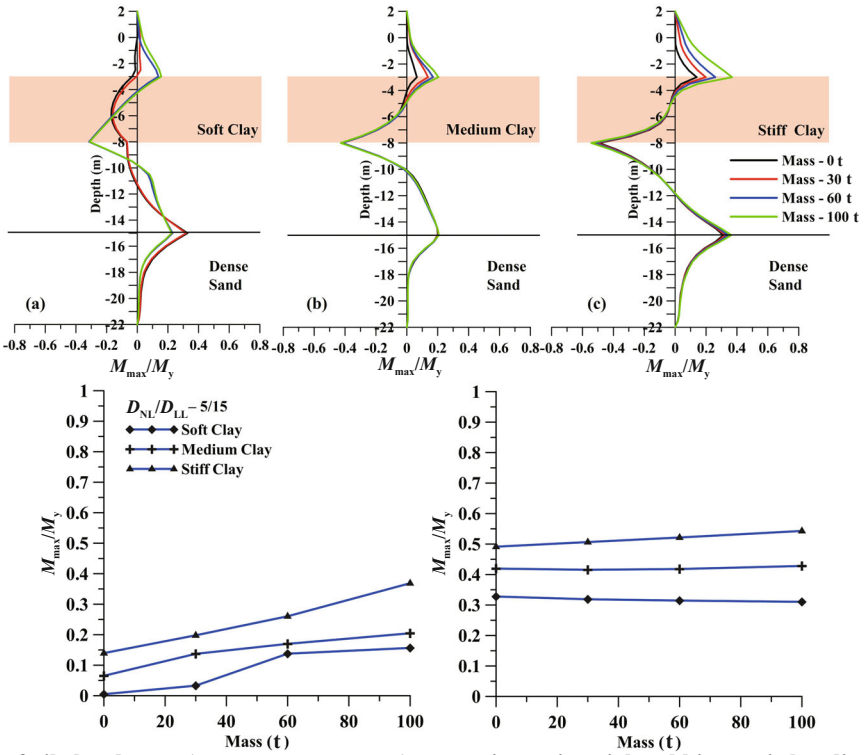

Fig. 16 Effect of pile head mass (superstructure mass) on maximum inertial and kinematic bending moment

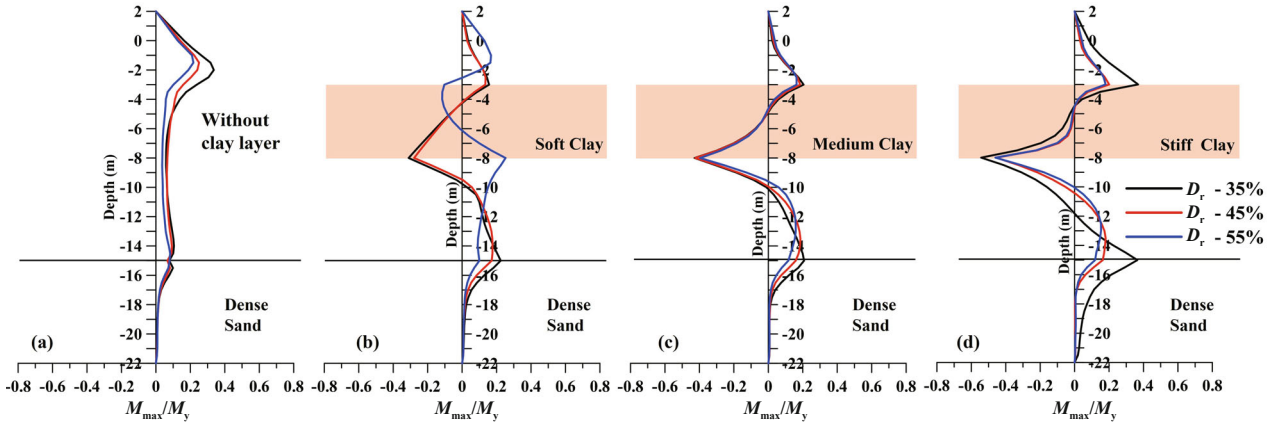

Fig. 17 Effect of relative densities of the liquefiable soil layer on the normalized maximum bending moment with depth

Figure 17(a) is for the case without any sandwiched non-liquefiable soil layer. It can be observed from Fig. 17(a) that the maximum bending moment has occurred in the top portion of the pile (due to inertia). An increase in soil relative density resulted in a lesser bending moment because of the increased soil stiffness. It can be observed from Figs. 17(b) and 17(c) that the effect of relative density is quite marginal in the case of soft and medium clay. However, in the case of stiff clay, the presence of high relative density soil reduces both inertial and kinematic effects on the pile due to the lesser stiffness contrast of the soil layers, as can be seen in Fig. 17(d).

3.8 Effect of position of non-liquefiable clay layer in liquefiable deposit on the bending moment of pile foundation

It is imperative from the observations that the sandwiched non-liquefiable clay layer influences the behavior of the pile foundation, including its thickness and position within the liquefiable layer. The previously discussed analyses had the location of the clay layer fixed, as shown in Fig. 1. Therefore, to quantify the effect of the position of the sandwiched clay layer on the bending moment of the pile foundation, its position is varied in the liquefiable soil deposit of 15 m. A representative sketch for a 5 m clay layer with varying positions is shown in Fig. 18. The study is conducted for the clay layer with thicknesses varying from 1 m to 14 m, and for all types of clay layers. The variation of normalized maximum bending moment for D_{NL}/D_{LL} – 5/15 is shown in Fig. 19 for input ground motion of the Kobe earthquake scaled to 0.2 g (several representative cases are plotted). It can be observed from Fig. 19 that as the position of the clay layer shifts away from the ground level, the position of the partial fixity effect also changes accordingly, as can be observed for medium and stiff clay cases. For the case of stiff clay, the kinematic bending moment of the pile foundation decreases as the position of the clay layer goes to a deeper depth. Figure 20 shows the variation of maximum inertial and kinematic bending moment in the pile as the clay layers shift away from the ground level for stiff clay layers of thicknesses of 3 m, 5 m, 7 m, and 9 m. As the position of the stiff clay shifts away from the ground level, the kinematic bending moment decreases, and the inertial bending moment increases except for the case of D_{NL}/D_{LL} = 7/15. It can also be observed from the figure that the governing bending moment for the pile design also depends on the position of the sandwiched clay layer. For the case of a stiff clay layer, a case is added where the clay layer is kept at 2 m below ground level to check the consistency of the results (only for the stiff clay case). It can be observed from both Figs. 19 and 20 that variation of the bending moment is consistent. Even though in most of the scenarios, the kinematic bending moment governs the pile design; however, it's advisable to check for inertia cases as well. Therefore, in geotechnical investigations, the thickness and location of non-liquefiable clay layers should be carefully determined, and its probable variation in position may suitably be considered for design.

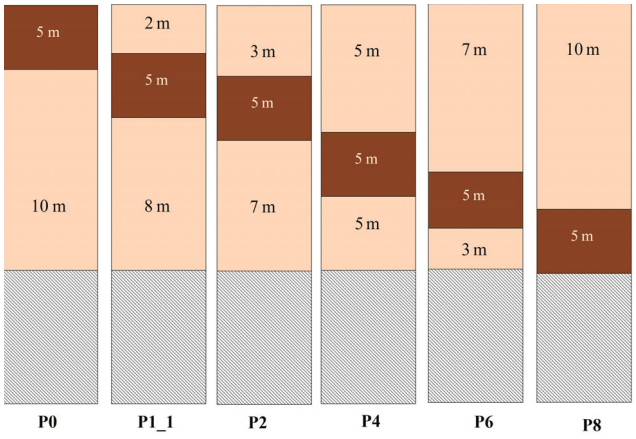

Fig. 18 Soil profiles considered in the study for effect of clay layer position

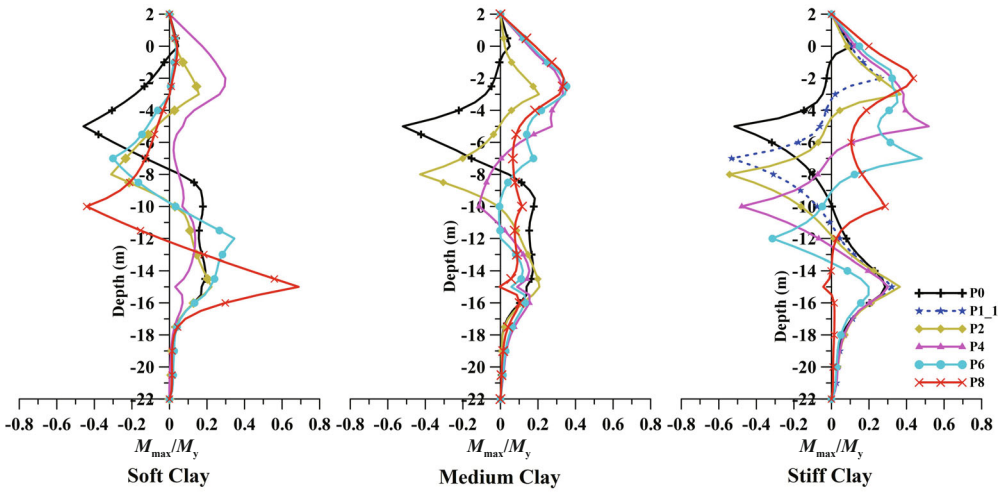

Fig. 19 Influence of the position of non-liquefiable soil (clay) layer on the maximum bending moment of pile foundation

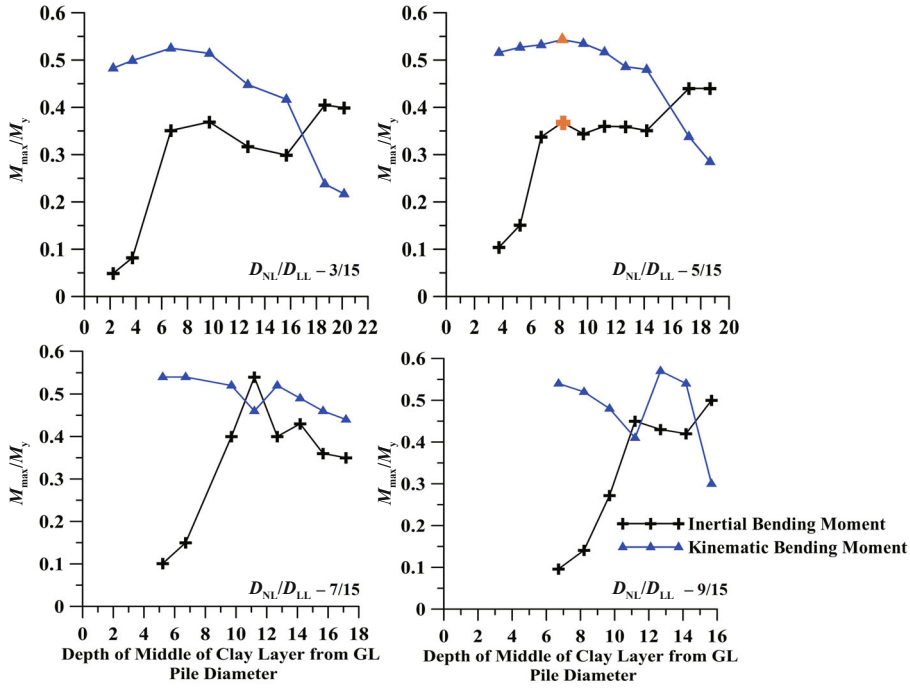

Fig. 20 Influence of the position of non-liquefiable soil (clay) layer – stiff clay layer on maximum kinematic and inertial bending moment

3.9 Comparison of the kinematic bending moment with empirical models

From the study presented above, it can be inferred that pile foundations in layered liquefiable soil deposits can have higher kinematic bending moments due to the seismic forces from inertial bending moments in some scenarios and should be given consideration during design. The majority of seismic design codes still do not guide how to estimate the kinematic bending moment for pile design. JRA (2003) code suggests neglecting the effect of the sandwiched clay (non-liquefiable) soil layer present in the liquefiable soil deposit. CEN (2004) requires consideration of the kinematic loading on the pile foundation under several circumstances. However, it does not recommend or specify any procedure to estimate the kinematic bending moment. Many researchers have made considerable efforts in understanding the inertial and kinematic effects and their interaction. Analytical, finite element, and scaled experimental studies have helped in formulating the procedure for estimating the kinematic bending moment on the pile foundation. Table 3 lists some of the available methods to estimate the kinematic bending moment suggested by Dobry and O'Rourke (1983), Nikolaou *et al*. (1995, 2001), and Di Laora *et al*. (2012). One soil profile (Fig. 1(e), i.e., D_{NL}/D_{LL}=5/15) is considered to verify the application of these formulations to estimate the kinematic bending moment, and the results are plotted in Fig. 21. It can be observed from Fig. 21 that for the case of soft clay, using the Di Laora *et al*. (2012) method, the kinematic bending moment is estimated reasonably close to the

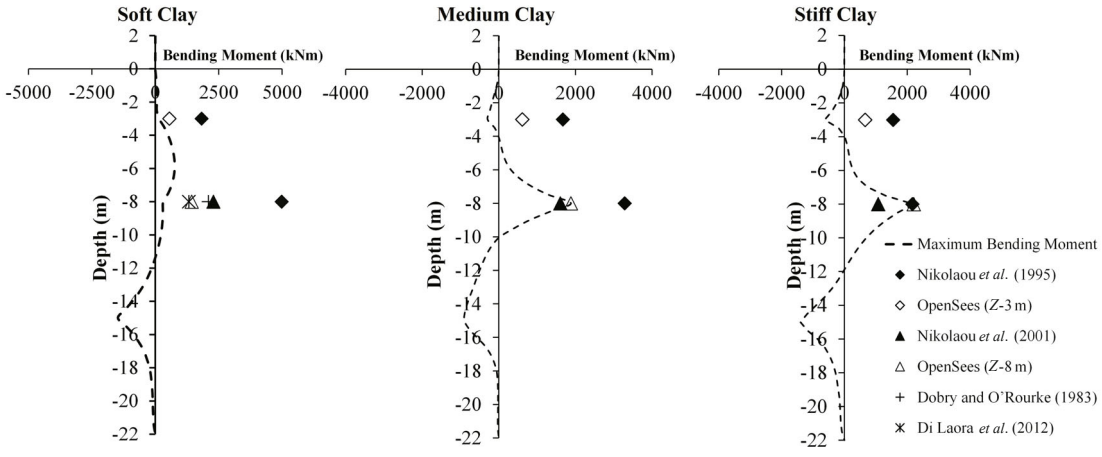

Fig. 21 Comparison of maximum kinematic bending moment of numerical evaluation with methods described in the literature

Table 3 Methods to estimate the kinematic bending moment

Author	Equation
Dobry and O'Rourke (1983)	$M_{\mathrm{k}} = 1.86(E_{\mathrm{P}}I_{\mathrm{P}})^{0.75}(G_1)^{0.25}\gamma_1 F$ $F = \dfrac{(1+c^{-4})(1+c^3)}{(1+c)(c^{-1}+1+c+c^2)}$ $c = \left(\dfrac{G_2}{G_1}\right)^{0.25}$ $\gamma_1 = \dfrac{r_{\mathrm{d}}\rho_1 h_1 a_{\mathrm{s}}}{G_1}$ $r_{\mathrm{d}} = 1 - 0.015z$
Nikolaou *et al*. (1995)	$M_{\max} = \dfrac{2.7}{10^7}E_{\mathrm{P}}d^3\left(\dfrac{a_{\mathrm{rock}}}{\mathrm{g}}\right)\left(\dfrac{L}{d}\right)^{1.30}\left(\dfrac{E_{\mathrm{P}}}{E_{\mathrm{I}}}\right)^{0.7}\left(\dfrac{V_2}{V_1}\right)^{0.3}\left(\dfrac{h_1}{L}\right)^{1.25}$ $M_{\mathrm{k}} = \eta_1 M_{\max}$
Nikolaou *et al*. (2001)	$M_{\mathrm{R}} = 0.042\tau_{\mathrm{c}}d^3\left(\dfrac{L}{d}\right)^{0.30}\left(\dfrac{E_{\mathrm{P}}}{E_{\mathrm{I}}}\right)^{0.65}\left(\dfrac{V_2}{V_1}\right)^{0.5}$ $\tau_{\mathrm{c}} = a_{\mathrm{s}}\rho_1 h_1$ $M_{\mathrm{k}} = \eta_2 M_{\mathrm{R}}$
Di Laora *et al*. (2012)	$M_{\mathrm{k}} = \dfrac{2E_{\mathrm{P}}I_{\mathrm{P}}}{d}\left(\dfrac{\varepsilon_{\mathrm{P}}}{\gamma_1}\right)\gamma_1$ $\left(\dfrac{\varepsilon_{\mathrm{P}}}{\gamma_1}\right) = \chi\left[-5\left(\dfrac{h_1}{d}\right)^{-1} + \left(\dfrac{E_{\mathrm{P}}}{E_{\mathrm{I}}}\right)^{-0.25}(c-1)^{0.5}\right]$ $\chi \cong 0.93$

numerically obtained value, as compared to the other methods. For the case of medium clay and stiff clay, the Nikolaou *et al*. (1995, 2001) method predicts the bending moment reasonably well, respectively. Note that these methods are based on the linear behavior of soil and are developed for two-layered soil deposits; at higher earthquake loads, soil behavior is expected to be highly nonlinear. Due to these constraints, Garala *et al*. (2020) suggested that these methods be used with a suitable modification to the soil properties.

4 Conclusions

In the present study, the response of pile foundations in alternate layered liquefiable and non-liquefiable soil deposits is investigated through a detailed numerical scheme. A parametric study is carried out to understand and quantify the effect of the sandwiched non-liquefiable soil layer on the response of end-bearing pile, and the major conclusions are presented below.

(1) With an increase in peak ground acceleration (PGA), both inertial and kinematic bending moments in the pile increase. However, in the presence of alternative layered liquefiable soil deposits, the kinematic response is significantly influenced by the PGA and frequency content of the input earthquake motion, as compared to the inertial response.

(2) Inertial bending moment mainly concentrates towards the top portion of the pile, whereas the kinematic bending moment is observed to be maximum at the bottom interface of the non-liquefied and liquefied soil layer for all the cases considered.

(3) Liquefiable soil layers of higher initial relative density reduce both inertial and kinematic bending moment on the pile foundation, as it offers higher lateral resistance.

(4) An increase in strength and thickness of the sandwiched non-liquefiable soil layer restrains the pile displacement, and the net pile head displacement reduces due to the presence of sandwiched non- liquefied soil.

(5) Typically, the design process for a pile foundation neglects the non-liquefied soil layer within a liquefiable soil deposit. However, when such foundations are placed in layered soil deposits, including layers of liquefiable soil, both inertial and kinematic bending moments could govern the design. It is necessary to employ appropriate empirical equations to estimate the kinematic bending moment of the pile. The design strength of the pile must be checked for both inertial and kinematic bending moments if it is placed in a liquefiable soil deposit that includes a sandwiched non-liquefiable layer.

Acknowledgment

The first author would like to thank The Ministry of Education, Government of India, for the financial assistance provided during the research work.

References

Abdoun T, Dobry R, O'Rourke TD and Goh SH (2003), "Pile Response to Lateral Spreads: Centrifuge Modelling," *Journal of Geotechnical and Geoenvironmental engineering,* **129**(10): 869–878. https://doi.org/10.1061/(ASCE)1090-0241(2003)129:10(869)

API (2005), *Recommended Practice for Planning, Designing, and Constructing Fixed Offshore Platforms-Working Stress Design*, 21st Ed., API RP 2A-WSD, Washington, DC: American Petroleum Institute.

Ashford SA and Juirnarongrit T (2002), "Response of Single Piles and Pipelines in Liquefaction-Induced Lateral Spreads Using Controlled Blasting," *Earthquake Engineering and Engineering Vibration*, **1**: 181–193. https://doi.org/10.1007/s11803-002-0064-3

Berrill J and Yasuda S (2002), "Liquefaction and Piled Foundations: Some Issues," *Journal of Earthquake Engineering*, **6**(S1): 1–41. https://doi.org/10.1080/13632460209350431

Bhattacharya S (2003), "Pile Instability During Earthquake Liquefaction," *Doctoral Dissertation*, University of Cambridge, UK.

Bhattacharya S, Bolton MD and Madabhushi SPG (2005), "A Reconsideration of the Safety of Piled Bridge Foundations in Liquefiable Soils," *Soils and foundations*, **45**(4): 13–25. https://doi.org/10.3208/sandf.45.4_13

Bhattacharya S and Goda K (2013), "Probabilistic Buckling Analysis of Axially Loaded Piles in Liquefiable Soils," *Soil Dynamics and Earthquake Engineering*, **45**: 13–24. https://doi.org/10.3208/sandf.45.4_13

Biot MA (1955), "Theory of Elasticity and Consolidation for a Porous Anisotropic Solid," *Journal of applied physics*, **26**(2): 182–185.

Boulanger RW, Curras CJ, Kutter BL, Wilson DW and Abghari A (1999), "Seismic Soil-Pile-Structure Interaction Experiments and Analyses," *Journal of Geotechnical and Geoenvironmental Engineering,* **125**(9): 750–759. https://doi.org/10.1061/(ASCE)1090-0241(1999)125:9(750)

Brandenberg SJ, Boulanger RW, Kutter B and Chang D (2005), "Behavior of Pile Foundations in Laterally Spreading Ground During Centrifuge Tests," *Journal of Geotechnical and Geoenvironmental Engineering*, **131**(11): 1378–1391. https://doi.org/10.1061/(ASCE)1090-0241(2005)131:11(1378)

CEN (2004), *EN 1998-5, Eurocode 8: Design of Structures for Earthquake Resistance – Part 5: Foundation Retaining Structures and Geotechnical Aspects*, Brussels, Belgium.

Cheng Z, Jeremić B (2009), "Numerical Modeling and Simulation of Pile in Liquefiable Soil," *Soil Dynamics and Earthquake Engineering*, **29**(11-12): 1405–1416. https://doi.org/10.1016/j.soildyn.2009.02.008

Cubrinovski M, Ishihara K and Poulos H (2009), "Pseudo-Static Analysis of Piles Subjected to Lateral Spreading," *Bulletin of the New Zealand Society for Earthquake Engineering*, **42**(1): 28–38. https://doi.org/10.5459/bnzsee.42.1.28-38

Dash SR and Bhattacharya S (2021), "Experimental *p-y* Curves for Liquefied Soils from Centrifuge Tests," *Earthquake Engineering and Engineering Vibration*, **20**: 863–876. https://doi.org/10.1007/s11803-021-2059-y

Dash SR, Bhattacharya S and Blakeborough A (2010), "Bending–Buckling Interaction as a Failure Mechanism of Piles in Liquefiable Soils," *Soil Dynamics and Earthquake Engineering*, **30**(1-2): 32–39. https://doi.org/10.1016/j.soildyn.2009.08.002

Davisson MT and Robinson KE (1965), "Bending and Buckling of Partially Embedded Piles," *Proceedings of the 6th ICDMFE*, (2): 243–246.

Di Laora R, Mandolini A and Mylonakis G (2012), "Insight on Kinematic Bending of Flexible Piles in Layered Soil," *Soil Dynamics and Earthquake Engineering*, **43**: 309–322. https://doi.org/10.1016/j.soildyn.2012.06.020

Dobry R and O'Rourke MJ (1983), "Discussion of 'Seismic Response of End-Bearing Piles' by Flores Berrones R. and Whitman R.V," *Journal of Geotechnical Engineering*, **109**(5): 778–781. https://doi.org/10.1061/(ASCE)0733-9410(1983)109:5(778)

FEMA 369 (2000), *NEHRP Recommended Provisions* (*National Earthquake Hazards Reduction Program*) *for Seismic Regulations for New Buildings and Other Structures. Part 2: Commentary*, Building Seismic Safety Council, USA.

Finn WDL and Fujita N (2002), "Piles in Liquefiable Soils: Seismic Analysis and Design Issues," *Soil Dynamics and Earthquake Engineering*, **22**(9-12): 731–742. https://doi.org/10.1016/S0267-7261(02)00094-5

Garala TK, Madabhushi GS and Di Laora R (2020), "Experimental Investigation of Kinematic Pile Bending in Layered Soils Using Dynamic Centrifuge Modelling," *Géotechnique*, 1–16. https://doi.org/10.1680/jgeot.19.P.185

Haldar S and Babu GLS (2010), "Failure Mechanisms of Pile Foundations in Liquefiable Soil: Parametric Study," *International Journal of Geomechanics*, **10**(2): 74–84. https://doi.org/10.1061/(ASCE)1532-3641(2010)10:2(74)

Haldar S, Babu GLS and Bhattacharya S (2008), "Buckling and Bending Response of Slender Piles in Liquefiable Soils During Earthquakes," *Geomechanics and Geoengineering*, **3**(2): 129–143. https://doi.org/10.1080/17486020802087101

Hamada M and O'Rourke TD (1992), "Case Studies of Liquefaction and Lifeline Performance during Past Earthquakes, Volume 1, Japanese Case Studies," *Technical Report*, National Center for Earthquake Engineering Research, USA.

Hardin BO and Drnevich VP (1972), "Shear Modulus and Damping in Soils: Measurement and Parameter Effects," *Journal of Soil Mechanics and Foundations Division*, **98**(6): 603–624.

Hui SQ, Tang L, Zhang XY, Wang YQ, Ling XZ and Xu BW (2018), "An Investigation of the Influence of Near-Fault Ground Motion Parameters on the Pile's Response in Liquefiable Soil," *Earthquake Engineering and Engineering Vibration*, **17**: 729–745. https://doi.org/10.1007/s11803-018-0472-7

IS 1893 (part-1), Code of Practice for Criteria for Earthquake Resistant Design of Structures," *Bureau of Indian Standards*, New Delhi 2016.

IS 2911-1-2, *Design and Construction of Pile Foundations, Part 1: Concrete Piles, Section 2: Bored Cast In-Situ Concrete Piles*, Bureau of Indian Standards, New Delhi 2010.

Janalizadeh A and Zahmatkesh A (2015), "Lateral Response of Pile Foundations in Liquefiable Soils," *Journal of Rock Mechanics and Geotechnical Engineering*, **7**(5): 532–539. https://doi.org/10.1016/j.jrmge.2015.05.001

Jia K, Xu CS, Du XL, Cui CY, Dou PF and Song J (2023), "Seismic Response Comparison and Sensitivity Analysis of Pile Foundation in Liquefiable and Non-Liquefiable Soils," *Earthquake Engineering and Engineering Vibration*, **22**(1): 87–104. https://doi.org/10.1007/s11803-023-2160-5

JRA (2003), *Specification for Highway Bridges, Part V Seismic Design*, Japanese Road Association, Japan.

Knappett JA and Madabhushi SPG (2009), "Influence of Axial Load on Lateral Pile Response in Liquefiable Soils, Part I: Physical Modelling," *Geotechnique*, **59**(7): 571–581. https://doi.org/10.1680/geot.8.009.3749

Li GJ and Motamed R (2017), "Finite Element Modeling of Soil-Pile Response Subjected to Liquefaction-Induced Lateral Spreading in a Large-Scale Shake Table Experiment," *Soil Dynamics and Earthquake Engineering*, **92**: 573–584. https://doi.org/10.1016/j.soildyn.2016.11.001

Liyanapathirana DS and Poulos HG (2005), "Seismic Lateral Response of Piles in Liquefying Soil," *Journal of Geotechnical and Geoenvironmental Engineering*, **131**(12): 1466–1479. https://doi.org/10.1061/(ASCE)1090-0241(2005)131:12(1466)

Lombardi D, Durante MG, Dash SR and Bhattacharya S (2010), "Fixity of Piles in Liquefiable Soils," *Proceedings of 5th International Conference on Recent Advances in Geotechnical Engineering and Soil Dynamics and Symposium in Honor of Professor IM Idriss*, 24–29.

Matlock H (1970), "Correlations for Design of Laterally Loaded Piles in Soft Clay," Offshore Technology in Civil Engineering's Hall of Fame Papers from the Early Years, 77–94.

McKenna F (2011), "OpenSees: A Framework for Earthquake Engineering Simulation," *Computer Science Engineering*, **13**(4): 58–66. https://doi.org/10.1109/MCSE.2011.66

Mohanty P, Dutta SC and Bhattacharya S (2017), "Proposed Mechanism for Mid-Span Failure of Pile Supported River Bridges During Seismic Liquefaction," *Soil Dynamics and Earthquake Engineering*, **102**: 41–45. https://doi.org/10.1016/j.soildyn.2017.08.013

Mohanty P, Xu D and Biswal S (2021), "A Shake Table Investigation of Dynamic Behavior of Pile Supported Bridges in Liquefiable Soil Deposits," *Earthquake Engineering and Engineering Vibration*, **20**: 1–24. https://doi.org/10.1007/s11803-021-2002-2

Nikolaou A, Mylonakis G and Gazetas G (1995), "Kinematic Bending Moments in Seismically Stressed Piles," *Technical Report No. NCEER-95-0022*, National Center for Earthquake Engineering Research, State University of New York, Buffalo, USA.

Nikolaou S, Mylonakis G, Gazetas G and Tazoh T (2001), "Kinematic Pile Bending During Earthquakes: Analysis and Field Measurements," *Géotechnique*, **51**(5): 425–440. https://doi.org/10.1680/geot.2001.51.5.425

Parker F and Reese LC (1970), "Experimental and Analytical Studies of Behavior of Single Piles in Sand Under Lateral and Axial Loading," *Research Report 117-2*, Center for Highway Research, The University of Texas at Austin, Austin, USA.

Simonelli AL, Di Sarno L, Durante MG, Sica S, Bhattacharya S, Dietz MS, Dihoru L, Taylor CA, Cairo R, Chidichimo A and Dente G (2014), "Experimental Assessment of Seismic Pile-Soil Interaction," *Seismic Evaluation and Rehabilitation of Structures*, 455–475. https://doi.org/10.1007/978-3-319-00458-7_26

Soga K (1998), "Soil Liquefaction Effects Observed in the Kobe Earthquake of 1995," *Proceedings of the Institution of Civil Engineers-Geotechnical Engineering*, **131**(1): 34–51.

Tang L, Ling XZ, Xu PJ, Gao X and Wang DS (2010), "Shake Table Test of Soil-Pile Groups-Bridge Structure Interaction in Liquefiable Ground," *Earthquake Engineering and Engineering Vibration*, **9**(1): 39–50. https://doi.org/10.1007/s11803-009-8131-7

Tang L, Maula BH, Ling XZ and Su L (2014), "Numerical Simulations of Shake-Table Experiment for Dynamic Soil-Pile-Structure Interaction in Liquefiable Soils," *Earthquake Engineering and Engineering Vibration*, **13**(1): 171–180. https://doi.org/10.1007/s11803-014-0221-53

Tang L, Zhang XY, Ling XZ, Li H and Ju NP (2016),

"Experimental and Numerical Investigation on the Dynamic Response of Pile Group in Liquefying Ground," *Earthquake Engineering and Engineering Vibration*, **15**(1): 103–114. https://doi.org/10.1007/s11803-016-0308-2

Tokimatsu K and Asaka Y (1998), "Effects of Liquefaction-Induced Ground Displacements on Pile Performance in the 1995 Hyogoken-Nambu Earthquake," *Soils and Foundations*, **38**: 163–177. https://doi.org/10.3208/sandf.38.Special_163

Tokimatsu K, Suzuki H and Sato M (2005), "Effects of Inertial and Kinematic Interaction on Seismic Behavior of Pile with Embedded Foundation," *Soil Dynamics and Earthquake Engineering*, **25**(7-10): 753–762. https://doi.org/10.1016/j.soildyn.2004.11.018

Wang XW, Luo FY, Su ZY and Ye AJ (2017), "Efficient Finite-Element Model for Seismic Response Estimation of Piles and Soils in Liquefied and Laterally Spreading Ground Considering Shear Localization," *International Journal of Geomechanics*, **17**(6): 06016039. https://doi.org/10.1061/(ASCE)GM.1943-5622.0000835

Wang XW, Ye AJ and Ji BH (2019a), "Fragility-Based Sensitivity Analysis on the Seismic Performance of Pile-Group-Supported Bridges in Liquefiable Ground Undergoing Scour Potentials," *Engineering Structures*, **198**: 109427. https://doi.org/10.1016/j.engstruct.2019.109427

Wang XW, Ye AJ, Shang Y and Zhou LX (2019b), "Shake-Table Investigation of Scoured RC Pile-Group-Supported Bridges in Liquefiable and Non-Liquefiable Soils," *Earthquake Engineering and Structural Dynamics*, **48**(11): 1217–1237. https://doi.org/10.1002/eqe.3186

Wang Y and Orense RP (2020), "Numerical Analysis of Seismic Performance of Inclined Piles in Liquefiable Sands," *Soil Dynamics and Earthquake Engineering*, **139**: 106274. https://doi.org/10.1016/j.soildyn.2020.106274

Wang YB, Zhang ZC, Wu XF and Zhu B (2023), "Centrifuge Tests for Seismic Response of Single Pile Foundation Supported Wind Turbines in Sand Influenced by Earthquake History," *Earthquake Engineering and Engineering Vibration*, **22**(3): 623–636. https://doi.org/10.1007/ s11803-023-2202-z

Wang ZH, Dueñas-Osorio L and Padgett JE (2013), "Seismic Response of a Bridge–Soil–Foundation System Under the Combined Effect of Vertical and Horizontal Ground Motions," *Earthquake Engineering and Structural Dynamics*, **42**(4): 545–564. https://doi.org/10.1002/eqe.2226

Wilson DW (1998), Soil-Pile-Superstructure Interaction in Liquefying Sand and Soft Clay, *Doctoral Dissertation*, University of California, Davis, USA.

Xu CS, Liu H, Dou PF, Wang JT, Chen S and Du XL (2023), "Analysis on Kinematic and Inertial Interaction in Liquefiable Soil-pile-structure Dynamic System," *Earthquake Engineering and Engineering Vibration*, **22**(3): 601–612. https://doi.org/10.1007/ s11803-023-2190-z

Yang Z (2000), "Numerical Modeling of Earthquake Site Response Including Dilation and Liquefaction," *PhD Thesis*, Columbia University, New York, USA.

Yang ZH, Elgamal A and Parra E (2003), "Computational Model for Cyclic Mobility and Associated Shear Deformation," *Journal of Geotechnical and Geoenvironmental Engineering*, **129**(12): 1119–1127. https://doi.org/10.1061/(ASCE)1090-0241(2003)129:12(1119)

Yoshida N and Hamada M (1990) "Damage to Foundation Piles and Deformation Pattern of Ground Due to Liquefaction-Induced Permanent Ground Deformations," *Proceedings of 3rd Japan-US Workshop on Earthquake Resistant Design of Lifeline Facilities and Countermeasures for Soil Liquefaction*, 147–161.

Yoshida N, Tazoh T, Wakamatsu K, Yasuda S, Towhata I, Nakazawa H and Kiku H (2007), "Causes of Showa Bridge Collapse in the 1964 Niigata Earthquake Based on Eyewitness Testimony," *Soils and Foundations*, **47**(6): 1075–1087. https://doi.org/10.3208/sandf.47.1075

Zhang J, Huo YL, Brandenberg SJ and Kashighandi P (2008), "Effects of Structural Characterizations on Fragility Functions of Bridges Subject to Seismic Shaking and Lateral Spreading," *Earthquake Engineering and Engineering Vibration*, **7**: 369–382. https://doi.org/10.1007/s11803-008-1009-2

Zhang J, Li YR, Rong X and Liang Y (2022a), "Dynamic *p-y* Curves for Vertical and Batter Pile Groups in Liquefied Sand," *Earthquake Engineering and Engineering Vibration*, **21**(3): 605–616. https://doi. org/10.1007/s11803-022-2107-2

Zhang J, Li YR, Yan ZX, Huang D, Rong X and Liang Y (2022b), "Experimental Study of Vertical and Batter Pile Groups in Saturated Sand Using a Centrifuge Shaking Table," *Earthquake Engineering and Engineering Vibration*, **21**(1): 23–36. https://doi.org/10.1007/s11803-021-2067-y

Zhang XR and Yang ZJ (2018), "Numerical Analyses of Pile Performance in Laterally Spreading Frozen Ground Crust Overlying Liquefiable Soils," *Earthquake Engineering and Engineering Vibration*, **17**(3): 491–499. https://doi.org/10.1007/s11803-018-0457-6

Zhang XY, Tang L, Ling XZ and Chan A (2020), "Critical Buckling Load of Pile in Liquefied Soil," *Soil Dynamics and Earthquake Engineering*, **135**: 106197. https://doi.org/10.1016/j.soildyn.2020.106197

List of symbols

a_{rock}	Accelerations at the bedrock level
a_s	Accelerations at the soil surface
d	Pile diameter
E_p	Young's moduli of the pile
E_2	Young's moduli of the topsoil layer
G_1	Shear moduli of topsoil layer
h_1	Thicknesses of the topsoil layer
I_p	Moment of inertia of pile (cross-sectional)
L	Length of the pile embedded in soil
M_k	Kinematic pile bending moment
M_{max}	Steady-state maximum kinematic pile bending moment
M_R	Harmonic steady-state pile bending moment under resonance conditions
V_1	Shear wave velocities of the top soil layers
V_2	Shear wave velocities of the bottom soil layers
z	Depth from the ground surface
r_d	Depth factor
γ_1	Shear strain in the top layer of the soil
ε_p	Pile bending strain
η_1 and η_2	Reduction factors
ρ_1	Mass density of the topsoil layer
τ_c	Characteristic shear stress in the topsoil layer
χ	Regression coefficient